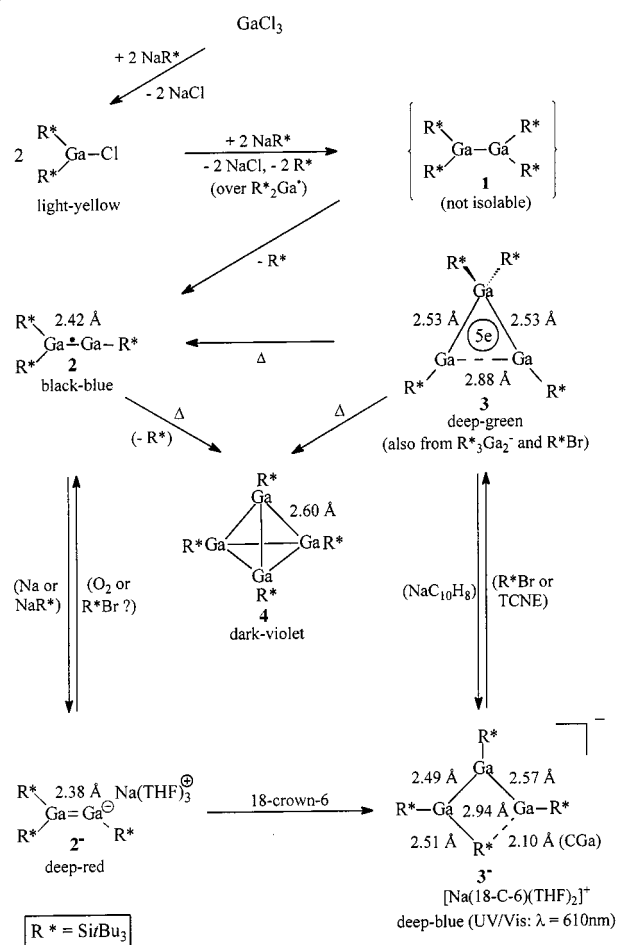


On the other hand, tetrakis(supersilyl)digallane $R^*_2Ga-GaR^*_2$ (**1**) thermolizes at much lower temperature than the dialane. Therefore, the reaction of gallium trichloride with supersilylsodium NaR^* in heptane at room temperature leads, via isolable bis(supersilyl)gallium chloride R^*_2GaCl , not at all to the digallane **1**, which is unknown to date, but directly to tris(supersilyl)digallanyl $R^*_3Ga_2^{\cdot}$ (**2**) (Scheme 2).^[3] The latter radicals thermolize in heptane at 100 °C exclusively to tetrakis(supersilyl)-*tetrahedro*-tetragallane $R^*_4Ga_4$ (**4**) (cf. preliminary communication^[4]). No tetrakis(supersilyl)cyclotrigallanyl $R^*_4Ga_3^{\cdot}$ (**3**) is formed in this case. Therefore, we tried to prepare the cyclotrigallanyl **2** by another route from the digallanyl **2**. These studies are presented here.



Scheme 2. Syntheses, reactions, colors, and Ga–Ga distances of gallanyl $R^*_3Ga_2^{\cdot}$ (**2**) and $R^*_4Ga_3^{\cdot}$ (**3**), gallanides $R^*_3Ga_2^-$ (**2**[−]) and $R^*_4Ga_3^-$ (**3**[−]) as well as tetrahedrane $R^*_4Ga_4$ (**4**) [equations in part not exactly formulated; R^* dimerizes to $(R^*)_2$ or – at higher temperatures – transforms into R^*H]

Results

Syntheses and Properties of $R^*_3Ga_2^{\cdot}$, $R^*_4Ga_3^{\cdot}$, $R^*_3Ga_2^-$, and $R^*_4Ga_3^-$

According to Scheme 2, the digallanyl $R^*_3Ga_2^{\cdot}$ (**2**) can be reduced in pentane, benzene, or tetrahydrofuran (THF)

with sodium in the presence or absence of naphthalene, or with supersilylsodium $NaR^* \times 2THF$ ($NaR^* \rightarrow Na^+ + R^* + e^-$) to sodium tris(supersilyl)digallanide–tetrahydrofuran(1/3) $[NaGa_2R^*_3 \times 3THF, 2^-; \text{cation } Na(THF)_3^+]$. In fact, one starts with bis(supersilyl)gallium chloride R^*_2GaCl , which is easily reduced by NaR^* or by $NaC_{10}H_8$ in THF. The digallanide **2**[−] forms deep-red, air- and moisture-sensitive crystals, which give red solutions in alkanes and benzene, but a blue solution in tetrahydrofuran (THF). The digallanide **2**[−] reacts in pentane with Me_3SiCl at low temperature with formation of light-red tris(supersilyl)(trimethylsilyl)digallane $[R^*_2Ga-GaR^*(SiMe_3); \text{evidence of the existence of a digallanide; first tetrasilyldigallane to date}]$.

If 18-crown-6 is added to a deep-red solution of **2**[−] in benzene, the color of the reaction mixture immediately changes to dark-blue. In fact, **2**[−] reacts according to Scheme 2 to give dark-blue, air- and moisture-sensitive sodium tetrakis(supersilyl)trigallanide–18-crown-6(1/1)–tetrahydrofuran(1/2) $\{[Na(18-C-6)(THF)_2]^+[Ga_3R^*_4]^- \}$, which is soluble in benzene and THF, but insoluble in alkanes (for X-ray structure analysis see below). Possibly, a transfer of supersilylgallium R^*Ga between two digallanide anions **2**[−] takes place as described by $2R^*_3Ga_2^- \rightarrow R^*_2Ga^- + R^*_4Ga_3^-$, whereby the monogallanide $R^*_2Ga^-$ may transfer another supersilylgallium by $R^*_2Ga^- + R^*_3Ga_2^- \rightarrow R^{*-} + R^*_4Ga_3^-$ (R^{*-} is unstable in the presence of 18-C-6 to produce R^*H).^[5]

The trigallanide $R^*_4Ga_3^{\cdot}$ (**3**[−]) is oxidized in benzene with supersilyl bromide ($R^*Br + e^- \rightarrow R^* + Br^-$) or tetracyanoethylene ($TCNE + 2e^- \rightarrow TCNE^{2-}$) to deep-green air- and moisture-sensitive, tetrakis(supersilyl)cyclotrigallanyl ($R^*_4Ga_3^{\cdot}$; **3**), soluble in organic media. The latter is itself reduced by sodium naphthalenide to $R^*_4Ga_3^-$ (cf. Scheme 2; for EPR spectrum and X-ray structure analysis see below). Unexpectedly, $R^*_4Ga_3^{\cdot}$ (**3**) besides $(R^*)_2$ is also very simply obtained by reaction of the digallanide $NaGa_2R^*_3 \times 3THF$ $\{Na(THF)_3^+ 2^-\}$ in pentane with supersilyl bromide R^*Br . As the radical **3** is formed faster from $R^*_3Ga_2^{\cdot}$ (**2**[−]) and R^*Br than from $R^*_4Ga_3^{\cdot}$ (**3**[−]) and R^*Br , the former reaction obviously does not proceed via anion **3**[−], but may involve the radical $R^*_3Ga_2^{\cdot}$ (**2**), which eventually reacts with **3**[−] by transfer of R^*Ga (cf. production of **3**[−] from **2**[−]).

Radical $R^*_4Ga_3^{\cdot}$ (**3**) thermolizes at 45 °C slowly (within 1 d) with formation of $R^*_3Ga_2^{\cdot}$, besides $R^*_4Ga_4$ (Scheme 2, cf. thermolysis of $R^*_4Al_3^{\cdot}$).^[6] The black-blue, air- and moisture-sensitive, in organic media soluble tris(supersilyl)digallanyl $R^*_3Ga_2^{\cdot}$ (**2**) is also synthesized in alkanes from $GaCl_3$ and NaR^* , or from R^*_2GaCl and NaR^* as well as Na ,^[3] or from $R^*_3Ga_2^{\cdot}$ (**2**[−]) by oxidation. Formally, the radical **3** decomposes with elimination of supersilylgallium R^*Ga into the digallanyl **2**, whereby R^*Ga tetramerizes. Because the digallanyl **2** itself decomposes at 100 °C in heptane to dark-violet air- and moisture-sensitive, in organic media soluble tetrakis(supersilyl)-*tetrahedro*-tetragallane ($R^*_4Ga_4$; **4**) and $(R^*)_2$,^[4] the trigallanyl **3** finally decomposes in pentane at 100 °C exclusively into $(R^*)_2$ and thermostable **4**

(almost no decomposition in solution at 100 °C; decomposition of the solid at the melting point 322 °C).

Characterization of $R^*_3Ga_2^{\cdot-}$, $R^*_4Ga_3^{\cdot-}$, $R^*_3Ga_2^-$, and $R^*_4Ga_3^-$

The ^{29}Si NMR signals of digallanide $[R^*_2Ga-GaR^*]^-$ [2^- ; the Ga–Na bond in $NaGa_2R^*_3 \times 3THF$ is according to the formulation $Na(THF)_3^+ 2^-$ undoubtedly ionic^[5]] and trigallanide $[R^*_2Ga-GaR^*-GaR^*]^-$ (3^-) appear at low field [$\delta = 37.1/54.3$ in the first case (area ratio ca. 2:1) and $\delta = 53.5/42.0/42.3$ in the second case (area ratio 2:1:1)]. The ^{29}Si NMR signals of the R^* groups in the digallane $R^*_2Ga-GaR^*(SiMe_3)$ show comparable shifts ($\delta = 48.80/44.80$ for 2 *Si*/Bu₃/1 *Si*/Bu₃). It is worth mentioning in this context that the ^{29}Si NMR signals of alkali metal supersil-anides MR* and of supersilyl halides R^*Hal appear in the same region at $\delta = 30-40$.^[5]

On the other hand, the radicals $R^*_3Ga_2^{\cdot-}$ (**2**) and $R^*_4Ga_3^{\cdot-}$ (**3**) – not observed in NMR – are characterized by EPR. As the EPR spectrum of **2** has been discussed in detail in a preliminary publication,^[3] the following remarks refer only to the EPR spectrum of **3**. Freshly dissolved in cyclohexane, **3** exhibits an unresolved, unsymmetrical EPR signal of $H_T \approx 20$ mT total width at $g = 1.998$. The lack of resolution and the asymmetry point to insufficient averaging of anisotropic contributions to the g and A (hyperfine) tensors. Similar, but less pronounced effects were observed for the paramagnetic systems $R^*_3Ga_2^{\cdot-}$ (**2**)^[3] and $R^*_4Ga_2^{\cdot-}$ with $R' = CH(SiMe_3)_2$.^[6a] In comparison with $R^*_4Al_3$ [¹] ($g = 2.0053$), the gallium analogue exhibits a g factor lower than $g(\text{electron}) = 2.0023$, which agrees^[7] with the presence of

low-lying unoccupied orbitals. On the other hand, a glassy frozen solution of **3** at 110 K in cyclohexane produces a broad ($H_T = 55$ mT), partially resolved EPR spectrum. While the signal could not be unambiguously analyzed due to overlapping g components in the X band, the large spectral width confirms the sizeable g and A anisotropy ($^{69}Ga:I = 3:2$, 60.1% natural abundance, isotropic hyperfine constant $a_0 = 435.68$ mT; $^{71}Ga:I = 3:2$, 39.9%, $a_0 = 553.58$ mT^[8]). The width of the low-temperature spectrum is in agreement with $H_T = 15.0$ mT for $R^*_4Al_3$ [¹] ($^{27}Al:I = 5:2$, 100%, $a_0 = 139.55$ mT^[8]). On prolonged standing or warming, the solution of **3** produces a new EPR signal that could be identified as that of **2**.^[3]

Structures of $R^*_3Ga_2^{\cdot-}$, $R^*_4Ga_3^{\cdot-}$, $R^*_3Ga_2^-$, and $R^*_4Ga_3^-$

The structures of the trigallanyl $R^*_4Ga_3^{\cdot-}$ (**3**), the digallanide $NaGa_2R^*_3 \times 3THF$ [2^- ; cation $Na(THF)_3^+$], and the trigallanide $[Ga_3R^*_4]^-$ [3^- ; cation $Na(18-C-6)(THF)_2^+$] are shown in the Figures 1, 2, and 3, respectively, together with selected bond lengths and angles. The structure of the digallanyl $R^*_3Ga_2^{\cdot-}$ (**2**) has already been published.^[3]

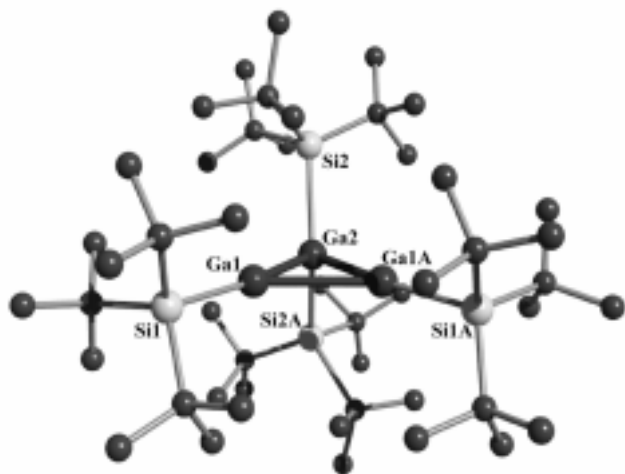


Figure 1. Structure of $R^*_4Ga_3^{\cdot-}$ (**3**) in the crystal; atom numbering used (SCHAKAL plot; H atoms omitted for clarity); selected distances [Å] and angles [°] with standard deviations: Ga1–Ga2 2.5267(7), Ga1–Ga1A 2.879(1), Ga1–Si1 2.513(1), Ga2–Si2A 2.536(1), Ga2–Si2 2.536(1), Si–C (mean value) 1.98; Si1–Ga1–Ga2 169.88(4), Si1–Ga1–Ga1A 134.83(3), Ga2–Ga1–Ga1A 55.27 (2) [angles sum at Ga1/Ga1A 359.98], Ga1–Ga2–Ga1A 69.47(3), Ga1–Ga2–Si2A 106.77(4), Ga1A–Ga2–Si2A 108.85(3), Ga1–Ga2–Si2 108.85(3), Ga1A–Ga2–Si2 106.77(4), Si2A–Ga2–Si2 136.30(7), C–Si–Ga (mean value) 108.62, C–Si–C (mean value) 111.99; Si2–Ga2–Ga1–Si1 81.97, Si1–Ga1–Ga1A–Si1A 1.67

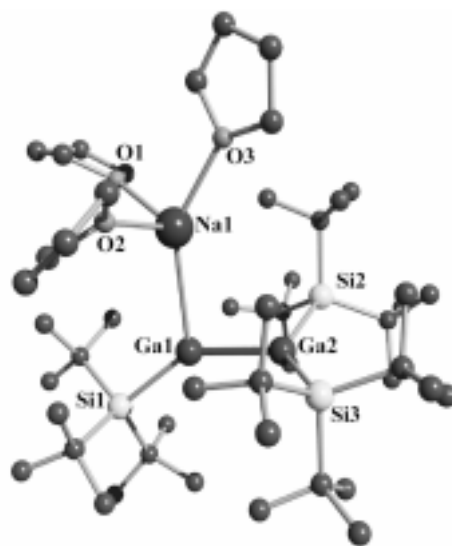


Figure 2. Structure of $NaGa_2R^*_3 \times 3THF$ [$Na(THF)_3^+ 2^-$] in the crystal; atom numbering used (SCHAKAL plot; H atoms omitted for clarity); selected distances [Å] and angles [°] with standard deviations: Ga1–Ga2 2.3797(6), Ga1–Si1 2.500(1), Ga1–Na1 3.205(2), Ga2–Si2 2.517 (1), Ga2–Si3 2.519(1), Na1–O3 2.316(4), Na1–O1 2.337(5), Na1–O2 2.404(5), Si–C (mean value) 1.96; Ga2–Ga1–Si1 142.41(4), Ga2–Ga1–Na1 91.40(4), Si1–Ga1–Na1 126.14(5) [angles sum at Ga1 359.94], Ga1–Ga2–Si2 112.09(3), Ga1–Ga2–Si3 112.59(3), Si2–Ga2–Si3 133.72(4) [angles sum at Ga2 358.34], O3–Na1–O1 91.3(2), O3–Na1–O2 88.1(2), O1–Na1–O2 97.6(2), O3–Na1–Ga1 112.9 (1), O1–Na1–Ga1 108.2 (1), O2–Na1–Ga1 145.7 (1), C–Si–Ga (mean value) 109.77, C–Si–C (mean value) 109.1; Si1–Ga1–Ga2–Si2/Si3 100.43/–91.99, Na1–Ga1–Ga2–Si2/Si3 82.52/–85.06

As stated elsewhere,^[3] the structure of tris(supersilyl)digallanyl ($R^*_3Ga_2^{\cdot-}$, **2**) is comparable with the structure of $R^*_3Al_2^{\cdot-}$. Both radicals show an almost planar Si_2E-ESi skeleton from which only the Si atom bonded to the biva-

lent E centre deviates by few degrees in line with the E–E vector (E = Al/Ga: 5.1/10°; the E–E–Si plane stands almost orthogonal to the Si–E–Si plane). In both cases, the E–E distance is comparatively short (cf. Schemes 1 and 2). This points to an E–E bonding order greater than one, whereby the shortening of the E–E bond length by going

from $R^*_3Al_2^{\cdot-}$ to $R^*_3Ga_2^{\cdot-}$ may be due to a decrease of the radius by going from Al atoms to Ga atoms. According to this, and in agreement with EPR studies,^[3,9] the radicals $R^*_3E_2^{\cdot-}$ contain sp^2 - and sp -hybridized E atoms, which are connected via two-electron δ - and one-electron π -bonds. This fact is best described by the formulation $R^*_2E-ER^{\cdot}$.

On the other hand, the structure of tetrakis(supersilyl)tri-gallanyl ($R^*_4Ga_3^{\cdot-}$, **3**), shown in Figure 1, is in many respects different from the structure of $R^*_4Al_3^{\cdot-}$ – except for the Si atoms of the 4 R^* groups which occupy in both radicals the corners of a distorted tetrahedron: In $R^*_4Al_3^{\cdot-}$ the three Al atoms occupy the corners of a triangle with two longer but unequal $R^*_2AlAIR^*$ sides and a shorter R^*AlAIR^* basis (cf. Scheme 1), whereas in $R^*_4Ga_3^{\cdot-}$ (**3**) the three gallium atoms form a triangle with two shorter and equal long $R^*_2GaGaR^*$ sides and a longer R^*GaGaR^* basis (cf. Scheme 2). These structural data suggest that the R^*Al groups are more weakly bonded to R^*_2Al than to each other, whereas the opposite holds for the R^*Ga groups. In addition, the R^*_2Al plane in $R^*_4Al_3^{\cdot-}$ stands not orthogonal to the E_3 plane and one R^* substituent of the R^*AlAIR^* group does not lie in the E_3 plane. This is unlike the R^*_2Ga plane in $R^*_4Ga_3^{\cdot-}$ (orthogonal to E_3) and the R^* substituents of the R^*GaGaR^* group (both in plane). Intuitively, one might argue that the observed geometry of both radicals looks as if cyclisation of the compounds *catena*- $R^*_2E-ER^{\cdot}-ER^{\cdot}$ (E = Al, Ga), which are homologues of the mentioned radicals *catena*- $R^*_2E-ER^{\cdot}$ (see above), stopped half way on the reaction coordinate in the case of $R^*_4Al_3^{\cdot-}$, but is finished in the case of $R^*_4Ga_3^{\cdot-}$. In the course of this (hypothetic) cyclisation of *catena*- $R^*_2E-ER^{\cdot}-ER^{\cdot}$ the R^*E-ER^{\cdot} bond became weaker and the connection between R^*_2E and ER^{\cdot} – not existing in *catena*- $R^*_4E_3^{\cdot-}$ – stronger.

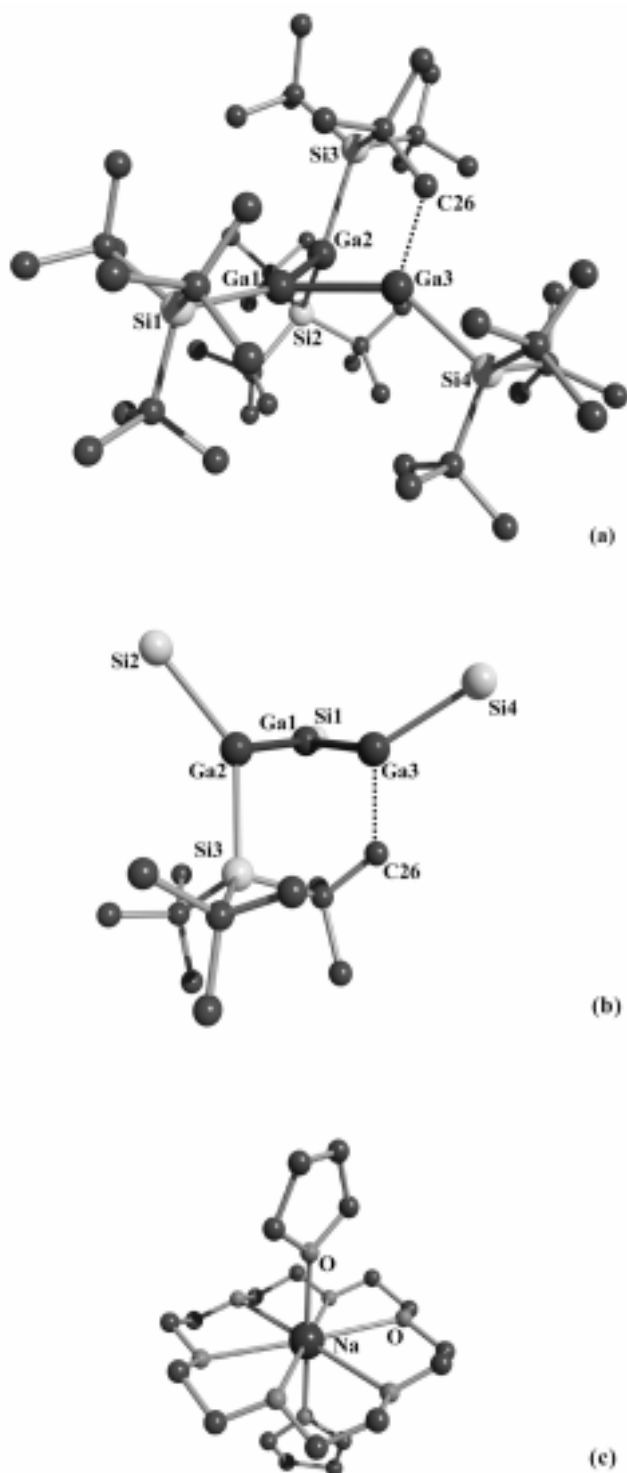


Figure 3. Structure of $R^*_4Ga_3^{\cdot-}$ (**3**[−]) in the crystal, seen in two directions [(a) and (b)], and of $Na(18-C-6)(THF)_2^+$ [(c)]; atom numbering used [SCHAKAL plot; H atoms in (a) and (b), and some *t*Bu groups in (b) omitted for clarity; the dotted lines represent the intramolecular $CH_3\cdots Ga$ contact]; selected distances [Å] and angles [°] with standard deviations: anion: Ga1–Ga3 2.494(1), Ga1–Ga2 2.569(2), Ga2 \cdots Ga3 2.935(2), Ga1–Si1 2.485(3), Ga2–Si3 2.513(3), Ga2–Si2 2.520(3), Ga3–Si4 2.486(3), Ga3 \cdots C26 2.10, Si–C (mean value) 1.96; Si1–Ga1–Ga3 137.89(9), Si1–Ga1–Ga2 151.09(8); Ga3–Ga1–Ga2 70.83(5) [angles sum at Ga1 359.81], Si3–Ga2–Si2 133.52(11), Si3–Ga2–Ga1 105.83(8), Si2–Ga2–Ga1 118.76(8) [angles sum at Ga2 358.11], Si4–Ga3–Ga1 136.28(8), Ga1–Ga3–C26 105.6(3), Si4–Ga3–C26 112.7(3) [angles sum at Ga3 354.6], Si4–Ga3–Ga2 140.19(8), Ga1–Ga3–Ga2 55.77(4), Ga1–Ga2–Ga3 53.40(4), C–Si–Ga (mean value) 109.39, C–Si–C (mean value) 109.5; Si2(Si3)–Ga2–Ga1–Si1 67.77/98.65, Si4–Ga3–Ga1–Si1 54.83, C26–Ga3–Ga1–Si1 95.84, Si2(Si3)–Ga2–Ga1–Ga3 117.91/75.67, Si4–Ga3–Ga1–Ga2 129.26, C26–Ga3–Ga1–Ga2 80.77; cation: Na–O(THF) (mean value) 2.31, Na–O(18-C-6) (mean value) 2.76; O–Na–O(THF) 179.24, O–Na–O(18-C-6) (mean value) 60.53, angles sum at O(THF) 359.78, angles sum at O(18-C-6) 343.40; the O_6 ring of 18-C-6 is something corrugated

If the R^*_2E group provides one and each R^*E group two electrons for the E_3 framework (Al, Ga), there are 5 electrons available for the E_3 cluster in $R^*_4E_3^-$ or $5/3 = 1.67$ electron per $E-E$ bond as compared with 3 electrons available for the E_2 group in $R^*_3E_2^-$. As a result, the mean value of the $E-E$ distances is evidently larger in $R^*_4E_3^-$ (2.74 Å for $R^*_4Al_3^-$, 2.65 Å for $R^*_4Ga_3^-$) than in $R^*_3E_2^-$ (2.53 Å for $R^*_3Al_2^-$, 2.42 Å for $R^*_3Ga_2^-$). Altogether one might expect that the groups R^*Ga in $R^*_4Ga_3^-$ are connected with R^*_2Ga by two-electron bonds, and among one another by a one-electron bond.

The structure of sodium tris(supersilyl)digallanide-tetrahydrofuran(1/3) $[NaGa_2R^*_3 \times 3THF, 2^-]$; cation: $Na(THF)_3^+$, shown in Figure 2, resembles that of the radical $R^*_3Ga_2^-$ (**2**; see above). Thus, in both molecules the Si_2GaGa groups are nearly planar (angles sum at Ga for **2** / **2** 358.4/359.7°). The same holds for the $GaGaNaSi$ group of the anion **2**⁻ (angles sum at Ga 360.0°), whereas the Na center itself is coordinated, distorted tetrahedrally by one Ga and three O atoms (the latter from THF). Moreover, the planes $Si-Ga-Si$ and $Ga-Ga-Si$ are almost orthogonal arranged not only in the anion **2**⁻ but also in the radical **2**. The $Ga-Ga-Si$ group in **2**⁻ is, however, far away from being linear (angles for **2**⁻/ **2** 142.4°/170.0°). This is obviously a consequence of the Na center, which in addition coordinates the Ga atom in **2**⁻. Certainly, the $Ga-Na$ bond, which runs nearly orthogonal to the $Ga-Ga$ bond (angle $Ga-Ga-Na$ 91.4°) is highly ionic. Therefore, the free electron pair at the anionic Ga atom of **2**⁻ is available for a π -bond, leading – according to the formulation $[R^*_2Ga-GaR^* \rightleftharpoons R^*_2Ga=GaR^*]^-$ – to a comparable short central bond of the anion ($Ga-Ga$ distance for **2**⁻/ **2** 2.38/2.42), approaching a bond order of 2 ($Ga=Ga$ double bond length ca. 2.32 Å; cf. Table 1).

In a way, the tris(supersilyl)digallanide $R^*_3Ga_2^-$ (**2**⁻) and tetrakis(supersilyl)trigallanide ($R^*_4Ga_3^-$) **3**⁻, the structure of the latter is now discussed (Figure 3, a), play the role of the second and third member in a homologous row of anions: $R^*_2Ga^-$, $R^*_2Ga-GaR^*$, $R^*_2Ga-GaR^*-GaR^*$, $R^*_2Ga-GaR^*-GaR^*-GaR^*$ {for the structure of $[Na(18-C-6)(THF)_2]^+$ cf. Figure 3 (c)}. In fact, the structure of the trigallanide **3**⁻ differs markedly from the structure of the digallanide **2**⁻ in showing an intramolecular H contact between one peripheral methyl group of the R^*_2Ga entity and the anionic Ga atom in $[R^*_2Ga-GaR^*-GaR^*]^-$ (cf. Scheme 2). As the contact between the C atom of the mentioned methyl group and gallium atom is also very short (2.10 Å; normal $Ga-C$ single bond lengths 1.99–2.02 Å),^[9] it seems not out of question that in addition to $H \cdots Ga$ contacts $C \cdots Ga$ contacts must be taken into account. The latter possibility is in good agreement with a comparable long R^*_2Ga $R^*Ga-GaR^*$ distance (2.57 Å), pointing to a $Ga-Ga$ single bond (cf. $Ga-Ga$ bond length of 2.38 Å in $R^*_2Ga-GaR^*$). Each of the three Ga atoms in $R^*_4Ga_3^-$ (**3**⁻) are nearly planar coordinated by adjacent atoms [angles sum at Ga for $Si_2GaGa/GaGaSiGa/GaGaSiC$ 358.1/359.9/354.8°; the angles between the mentioned planes are 82.89/76.20°; cf. Figure 3 (b)]. The Ga atoms in

3⁻ themselves occupy the corners of a triangle with two shorter sides and a much longer basis, which certainly do not represent any chemical bond (cf. Scheme 2). In regard to the central Ga_3 group in $[R^{*(2)}R^{*(3)}Ga-GaR^{*(1)}-GaR^{*(4)}]^-$ the supersilyl groups $R^{*(1)}/R^{*(2)}/R^{*(3)}/R^{*(4)}$ lie – according to Figure 3 (b) – in/below/above/below the Ga_3 plane; thereby the Si atoms of the 4 R^* groups form a distorted tetrahedron.

The one-electron reduction of the trigallanyl $R^*_4Ga_3^-$ (**3**) to $R^*_4Ga_3^-$ (**3**⁻) is connected with a structural change (anticyclization process), whereby the bonds $R^*_2Ga-GaR^*$ according to Figure 3 (b) – in/below/above/below the Ga_3 Scheme 2). Altogether, the mentioned reduction leads to a shortening of the mean $Ga-Ga$ distances $[(2.53 + 2.53 + 2.88):3 = 2.65$ Å in **3** and $(2.49 + 2.57):2 = 2.53$ Å in **3**⁻], but the $Ga-Ga$ distances in **3**⁻ are distinctly longer than in **2**⁻. This could be due to the fact that in the former the free electron pair contacts a methyl group $[-CH_3 \cdots Ga < \rightleftharpoons -CH_2-GaH <]$, whereas in the latter the free electron is involved in the $Ga-Ga$ bond $[>Ga-Ga' \rightleftharpoons >Ga \div Ga']$. On the other hand, the longer $Ga-Ga$ bonds perhaps are simply due to the fact that the extra electron is delocalised over three instead of over two Ga centers such as in **2**⁻.

Concluding Remarks

The gallium cluster compounds discussed here are further examples of many known compounds with two connected Ga atoms and of some known compounds with three connected Ga atoms.^[6,10–25] All these clusters are shown in Table 1, together with their colors and geometries [the bond orders are determined from the single and double $Ga-Ga$ bond lengths (2.52 and 2.32 Å), which themselves are twice the single and double bond radius of $Ga^{[26]}$].

According to Table 1, the $Ga-Ga$ bond lengths of organyl and certainly also of silyl-substituted digallanes $>Ga-Ga<$ with a two-electron $Ga-Ga$ bond (bond order 1) and tricoordinated Ga atoms span the region 2.48–2.54 Å. Clearly, the $Ga-Ga$ distances of the discussed digallanide $R_3Ga_2^-$ ($R = R^*$) or digallanediide $R_2Ga_2^{2-}$ [$R = 2,6-(Tip)_2C_6H_3$] as well as of the digallanyl $R_3Ga_2^-$ ($R = R^*$) or the radical anion $R_4Ga_2^{•-}$ [$R = Tip, (SiMe_3)_2CH$], which formally derive from R_4Ga_2 by removing one or two R^+ cations or one R^{\cdot} radical as well as introducing one electron, are distinctly shorter, due to the presence of more than two electrons per $Ga-Ga$ bond, leading to bond orders of 1.5 to 2, respectively (cf. Table 1). Obviously, substitution of the organyl substituents in R_4Ga_2 by more electronegative groups, shortens the $Ga-Ga$ bonds, as is shown for $(2,4,6-tBu_3C_6H_2)_2Ga_2Cl_2$ (Table 1). The yet unknown monomeric tetrahalides Ga_2Hal_4 should have – due to *electronic effects* of 4 halogen atoms – very short $Ga-Ga$ bond lengths. The comparable long $Ga-Ga$ bond in R_4Ga_2 with four electronegative substituents $R = 2,2,4,4-Me_4C_5H_6N$ probably is due to *steric effects*. On the other hand, addition of two donors to digallanes $>Ga-Ga<$ with formation of tetracoordinated Ga atoms certainly lengthens the $Ga-Ga$ bonds.

Table 1. Compounds with clusters of two and three Ga atoms [R = organyl, silyl, aminyl. X = halogen; D = donor; Fo = formula; CN = coordination number of Ga atoms (including Ga-bonded counter ions); τ = torsion angle R–Ga–Ga–R; BL = Ga–Ga bond length; BO = Ga–Ga bond order, determined from Ga–Ga single bond (2.52 Å) and double bond (2.32 Å); Ref. = references (here = this publication)]

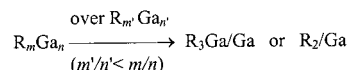
Fo	Ga cluster compounds		CN	τ [°]	BL [Å]	BO (ca.)	Ref.
	R/X/D ^[a]	Color ^[b]					
<i>Two Ga atoms</i>							
R ₄ Ga ₂	Disyl	yellow	3	4.9°	2.54	1	[10]
	Pip	lyellow	3	31°	2.53	1	[11]
	Tip	yellow	3	43.8°	2.51	1	[12]
	Mes _F	?	3	?	2.48	1	[13,14]
	3R*/SiMe ₃ ^[d]	red	3	?	?	?	here [15]
R ₂ Ga ₂ X ₂	Mes*/Cl	colorl.	3	0°	2.42	1.5	[16]
	R'/Cl	colorl.	4	e	2.50	1	[17]
	R'/Br	colorl.	4	e	2.51	1	[17]
Ga ₂ X ₄ D ₂	I/NET ₃	colorl.	4	st	2.50	1	[18]
	I/PEt ₃	colorl.	4	st	2.44	1.5	[18]
	Cl/Diox	colorl.	4	st	2.41	1.5	[19]
	Br/Diox	colorl.	4	st	2.40	1.5	[19]
	Cl/Py	colorl.	4	st	2.50	1.5	[20]
R ₂ Ga ₂ X ₄ ²⁻	Br/Py	colorl.	4	st	2.48	1.5	[20]
	R'/Br	colorl.	4	st	2.50	1	[17]
	R'/I	yellow	4	st	2.48	1	[17]
Ga ₂ X ₆ ²⁻ ^[f]	Cl	colorl.	4	st	2.43	1.5	[21]
	Br	colorl.	4	st	to ^[e]	to	to
	I	yellow	4	st	2.39	1.7	[23]
R ₃ Ga ₂ [•] (2)	R*	dblue	3+2	90°	2.42	1.5	here
R ₃ Ga ₂ ⁻ (2 ⁻)	R*	dred	3	90°	2.38	1.7	here
R ₂ Ga ₂ ⁻	[g]	dred	6	—	2.34	2	[14]
R ₄ Ga ₂ ⁻	Tip	dark	3	15.5°	2.34	2	[12]
R ₂ Ga ₂ ²⁻	Disyl	blue	3	0°	2.40	1.5	[6a]
	[h]	dred	4	180°	2.32	2	[24]
<i>Three Ga atoms</i>							
R ₄ Ga ₃ [•] (3)	R*	dgreen	3+4	—	2.54 ^[i]	1	here
R ₄ Ga ₃ ⁻ (3 ⁻)	R*	dblue	3	—	2.54 ^[i]	1	here
Ga ₃ I ₅ D ₃	PEt ₃	yellow	4	—	2.46	1.5	[18]
R ₃ Ga ₃ ²⁻	[k]	dred	4	—	2.44	1.5	[25]

[a] Disyl = (SiMe₃)₂CH; Pip = 2,2,4,4-Me₄C₅H₆N; Tip = 2,4,6-*i*Pr₃C₆H₂; Mes = 2,4,6-Me₃C₆H₂; Mes_F = 2,4,6-(CF₃)₃C₆H₂; R* = *t*Bu₃Si; Mes* = 2,4,6-*t*Bu₃C₆H₂; R' = (SiMe₃)₃Si; Diox = dioxane; Py = pyridine. — [b] d = deep, dark; l = light. — [c] st = staggered; e = eclipsed. — [d] R = [—*t*BuN—SiMe(N*t*Bu)—N*t*Bu—SiMe(N*t*Bu)—]. — [e] Ga–Ga bond lengths slightly depend on the counter ion. — [f] The gallium(II) chalcogenides GaY also contain Ga–Ga groups with tetracoordinated Ga atoms and Ga–Ga distances of 2.447/2.456/2.437 Å (Y = S/Se/Te). — [g] R = 2,4-bis(trimethylsilyl)-2,4-dicarba-*nido*-hexaboryl. — [h] R = 2,6-(Tip)₂C₆H₃. — [i] Mean value of the two shorter Ga–Ga bonds (cf. Scheme 2). — [k] R = 2,6-(Mes)₂C₆H₃.

As to Table 1, this “coordination effect” is or might be observed by going from R₂Ga₂Hal₂ (R = 2,4,6-*t*Bu₃C₆H₂) to [R₂Ga₂Hal₄]⁻ [R = Si(SiMe₃)₃] or from Ga₂Hal₄ (unknown) to [Ga₂Hal₆]²⁻.

Unlike triorganylgallium compounds R₃Ga with gallium in oxidation state III, which have been known for a long time,^[27] organylgallium compounds R_mGa_n with gallium in oxidation states < III were synthesized and characterized only very recently. This is due to their high tendency of decomposition into R₃Ga and Ga. According to the follow-

ing equation, the disproportionation of the mentioned gallium cluster compounds R_mGa_n – where R is not only an organic but also an inorganic group [e.g. (SiMe₃)₂N] – may proceed over intermediates R_{m'}Ga_{n'} with constantly decreasing *m*'/*n*' ratio.



Substituents R with *greater bulkiness* may inhibit the full scale of this disproportionation at a point which will be specifically determined by the nature of R and the reaction conditions (suitable donors that coordinate with Ga atoms of R_mGa_n may also have a directing effect). This is illustrated by the discussed reaction of gallium trihalides GaHal₃ with supersilylsodium NaR*, which according to Scheme 2 leads via R*₂GaCl to the digallanyl R*₃Ga₂[•] (2). The latter is metastable at room temperature, but at higher temperatures disproportionates further into R* and the *tetrahedro*-tetragallane R*₄Ga₄ (4; cf. Scheme 2). Obviously, the Ga₄ tetrahedrane in R*₄Ga₄ is completely shielded by four supersilyl groups, leading to a high thermal stability of the Ga cluster compound (see above). In accordance with this, the trigallanyl R*₄Ga₃[•] (3) finally – at elevated temperatures – disproportionates into R* and 4 (cf. Scheme 2).^[6] Certainly, 4 reacts further with Na in THF under formation of Na₂Ga₄R*₄ × 2THF.^[28]

It is worth mentioning in this context that gallium monohalides GaHal react with supersilylsodium in a different manner to gallium trihalides. Products are the gallanides R*₆Ga₁₀⁻ and R*₆Ga₁₃⁻ besides R*₄Ga₄^[17] as well as the gallanes R*₈Ga₁₈ and R*₈Ga₂₂.^[29] Noticeable, in the course of reactions of NaR* with GaHal₃ the products obtained have equal or more supersilyl groups than Ga atoms, whereas reactions of NaR* with GaHal lead to products with equal or less supersilyl groups than Ga atoms. Certainly, this is due to different reaction paths, the nature of which have to be investigated.

Some insights into the mechanisms of the building up of clusters come from the isolated primary and secondary products of the reaction of NaR* with GaHal₃. Here, the efficiency of supersilylsodium for acting as reducing agent (R*₂GaCl + NaR* → R*₂Ga[•] + NaCl + R* and R*₃Ga₂[•] + NaR* → NaGa₂R*₃ + R*) as well as the tendency of the gallium cluster compounds for elimination of R* (R*₄Ga₂ → R*₃Ga₂[•] + R*) or transferring group R*Ga (2 Ga₂R*₃⁻ → GaR*₂⁻ + Ga₃R*₄⁻) is important. Certainly, supersilylgallium R*Ga also plays an essential part in the reaction of NaR* and GaHal. The gallylene, which is obviously obtained by supersilylanidation of GaHal, may combine with GaHal, whereby dehalogenations as well as R* eliminations of the formed Ga cluster compounds will produce “naked” Ga atoms in the cluster. These latter clusters may themselves be reduced by NaR* to anions, which may react with GaHal by introducing new “naked” Ga atoms into the Ga cluster framework.

Experimental Section

All experiments were carried out in flame-dried glass apparatus with standard Schlenk techniques under dry argon or nitrogen. During all manipulations, air and moisture were strictly excluded. The solvents (pentane, heptane, THF, C_6D_6 , C_6D_{12}) were distilled from sodium/lead or sodium/benzophenone. Available for use were: $GaCl_3$, Na, Me_3SiCl , 18-crown-6, TCNE (tetracyanoethylene). The following compounds were synthesized according to literature procedures: $NaR^* \times 2THF$,^[5] R^*_2GaCl ,^[30] $NaC_{10}H_8$ (sodium naphthalenide) in THF.^[31] – For NMR spectra a Jeol GSX-270 ($^1H/^{13}C/^{29}Si$: 270.17/67.94/53.67 MHz) and Jeol EX-400 ($^1H/^{13}C/^{29}Si$: 399.78/100.54/79.43 MHz) were available. The ^{29}Si NMR spectra were recorded with the INEPT or DEPT pulse sequence using empirically optimized parameters for the mentioned groups. – The EPR spectra were recorded with a Bruker System ESP 300.

Syntheses and Reactions of 2. – (i): A solution of $NaR^* \times 2THF$ (0.826 mmol) in heptane (15 mL) was added dropwise to a solution of R^*_2GaCl (0.208 g, 0.413 mmol) in heptane (10 mL) at $-78^\circ C$. As the mixture warmed to room temperature, the color of the initially formed yellow solution (R^*_2GaCl , NaR^*) changed to green, and finally to intense blue. According to 1H NMR (exchange of heptane by C_6D_6) and to EPR, the solution contained $(R^*)_2$ and the radical **2**. The former substance is not observed by EPR, the latter not in NMR. After removal of the volatile components (ca. 10^{-3} mbar), the residue was placed in pentane (10 mL), the white precipitate (NaCl) removed by filtration, and the resulting solution reduced in volume to about 5 mL. Within 0.5 d at $-23^\circ C$, colorless crystals of $(R^*)_2$ precipitated which were removed by decanting the blue solution. Black-blue crystals of air- and water-sensitive **2** – which at about $80^\circ C$ thermolize under formation of the tetrahydride **4**^[4] and react with Na or NaR^* in organic solvents under formation of $Na(THF)_3^+ 2^-$ – form from the mother liquor after 5 d at $-23^\circ C$ (ca. 10%). The identification of products results from comparison with authentic samples of $(R^*)_2$ ^[5] and **2**.^[3] – (ii): The radical **2** is also formed from $GaCl_3$ and $NaR^* \times 2THF$ (molar ratio 1:3) in heptane.^[3] In addition, the digallanyl **2** seems – according to EPR – to be the first product of the oxidation of 2^- with oxygen. Finally, **2** probably is formed as first product of the reaction of $Na(THF)_2^+ 2^-$ in pentane with R^*Br (see below).

Syntheses and Reactions of $Na(THF)_3^+ 2^-$. – (i): A solution of $NaR^* \times 2THF$ (3.58 mmol) in THF (6 mL)/pentane (10 mL) was added dropwise to a solution of R^*_2GaCl (0.902 g, 1.79 mmol) in pentane (50 mL). The color of the initially yellow solution (R^*_2GaCl) changed to green and finally to dark-blue. According to 1H NMR (exchange of pentane by C_6D_6), the solution contained $(R^*)_2$ ^[5] and $Na(THF)_3^+ 2^-$ [molar ratio ca. 2:1; $2 R^*_2GaCl + 3 NaR^* \rightarrow Na^+ 2^- + 2 (R^*)_2 + 2 NaCl$] besides unreacted $NaR^* \times 2THF$ (all R^*_2GaCl consumed). After removal of the volatile components (ca. 10^{-3} mbar), the residue (now brown-red) was placed in pentane (50 mL), the precipitate (NaCl) removed by filtration, and the resulting dark-red solution reduced in volume to about 15 mL. Within 1 d at $-23^\circ C$, deep-red crystals of air- and water-sensitive $Na(THF)_3^+ 2^-$ (0.22 g; 0.26 mmol; 15%) formed from the solution, which reacted with Me_3SiCl and R^*Br (see below). – 1H NMR (C_6D_6 , internal TMS): δ = 1.47 (broad; 3 $SiBu_3$), 1.34/3.42 (m/m; 6- CH_2CH_2O /6- CH_2CH_2O). – $^{13}C\{^1H\}$ NMR (C_6D_6 , internal TMS): δ = 24.3/25.3 (6- CMe_3 /6- CMe_3), 33.2/33.9 (3- CMe_3 /3- CMe_3), 25.6/67.9 (6- CH_2CH_2O /6- CH_2CH_2O). – $^{29}Si\{^1H\}$ NMR (C_6D_6 , external TMS): δ = 37.1 (2 $SiBu_3$), 54.3 ($SiBu_3$). – X-ray structure analysis: cf. Figure 2. – It has not yet been possible to obtain a satisfactory elemental analysis. – (ii):

$NaC_{10}H_8$ (0.272 mmol) in THF (5 mL) was added dropwise to a solution of R^*_2GaCl (0.092 g; 0.181 mmol) in heptane (10 mL) at $-78^\circ C$. The color of the initially yellow solution (R^*_2GaCl) changed to violet (**2**) and finally brown-red $[Na(THF)_3^+ 2^-]$. After 6 h, the reaction mixture was warmed to room temperature. According to 1H NMR (exchange of THF/pentane by C_6D_6) the solution contained $(R^*)_2$ ^[5] and the digallanide $Na(THF)_3^+ 2^-$ [molar ratio 1:2; $2 R^*_2GaCl + 3 Na \rightarrow Na^+ 2^- + 0.5 (R^*)_2 + 2 NaCl$]. After removal of the volatile components (ca. 10^{-3} mbar), the residue (brown-red) was placed in heptane (30 mL), the precipitate (NaCl) removed by filtration, and the resulting dark-red solution reduced in volume to 5 mL. Within 1 d at $-23^\circ C$, deep-red crystals of $Na(THF)_3^+ 2^-$ (0.064 g; 0.066 mmol; 73%) formed from the solution [cf. (i) for characterization]. – (iii): In an NMR tube the radical **2** (ca. 0.015 g; 0.02 mmol) and Na (ca. 0.9 mmol) in C_6D_6 (0.6 mL) were heated for 1 d at $60^\circ C$. The color of the initially intensive blue solution changed finally to red. According to 1H NMR it contained $(R^*)_2$ ^[5] besides the digallanide $Na^+ 2^-$ (doubtless as the benzene adduct). – 1H NMR (C_6D_6 , internal TMS): δ = 1.421 (s; 2 $SiBu_3$), 1.434 (s; $SiBu_3$). – (iv) **Reaction of $Na(THF)_3^+ 2^-$ with Me_3SiCl :** A solution of Me_3SiCl (0.220 mmol) in heptane (5 mL) was added dropwise to a solution of $Na(THF)_3^+ 2^-$ (0.215 g; 0.220 mmol) in heptane (10 mL). The color of the initially formed dark-blue solution of the starting material changed to light-red. After removal of the volatile components at $-78^\circ C$ and ca. 10^{-3} mbar, the residue was warmed to room temperature and dissolved in C_6D_6 . According to NMR spectra, $Na(THF)_3^+ 2^-$ has exclusively reacted under formation of a new substance, the nature of which is probably the digallane $R^*_2Ga-GaR^*(SiMe_3)$. – 1H NMR (C_6D_6 , internal TMS): δ = 0.173 (s; $SiMe_3$), 1.258 (s; $SiBu_3$), 2.277 (s; 2 $SiBu_3$). – $^{13}C\{^1H\}$ NMR (C_6D_6 , internal TMS): δ = 1.29 ($SiMe_3$), 25.4/25.6 (6- CMe_3 /3- CMe_3), 32.4/33.9 (6- CMe_3 /3- CMe_3). – $^{29}Si\{^1H\}$ NMR (C_6D_6 , external TMS): δ = 19.41 ($SiMe_3$), 44.80 ($SiBu_3$), 48.42 (2 $SiBu_3$).

Syntheses and Reactions of $[Na(18-C-6)(THF)_2]^+ [3]^-$. – (i): To a solution of $Na(THF)_3^+ 2^-$ (0.147 g; 0.15 mmol) in 0.6 mL of C_6D_6 at room temperature was added 18-crown-6 (0.053 g; 0.20 mmol). The color of the initially red solution immediately changed to dark-blue. According to NMR recorded after 20 h, the trigallanide $[Na(18-C-6)(THF)_2]^+ [3]^-$ had formed. From this solution at $5^\circ C$ within 2 weeks dark-blue, air- and moisture-sensitive crystals of $[Na(18-C-6)(THF)_2]^+ [3]^-$, insoluble in pentane and soluble in benzene or THF, and which may be oxidized by R^*Br or TCNE under formation of the radical **3** (see below), were obtained. – 1H NMR (C_6D_6 , internal TMS): δ = 1.532 (broad; 2 $SiBu_3$), 1.621 (broad; 2 $SiBu_3$), 1.439/3.545 (m/m; 4- CH_2CH_2O /4- CH_2CH_2O), 3.326 (18-C-6). – $^{13}C\{^1H\}$ NMR (C_6D_6 , internal TMS): δ = 22.7/24.9 (6- CMe_3 /6- CMe_3), 32.2/35.0 (6- CMe_3 /6- CMe_3), 25.8/67.8 (4- CH_2CH_2O /4- CH_2CH_2O), 70.0 (18-C-6). – $^{29}Si\{^1H\}$ NMR (C_6D_6 , external TMS): δ = 42.0/42.3/53.2 ($SiBu_3$ / $SiBu_3$ /2 $SiBu_3$). – X-ray structure analysis: cf. Figure 3. – It has not yet been possible to obtain a satisfactory elemental analysis. – (ii): Deep-blue $[Na(18-C-6)(THF)_2]^+ [3]^-$ was formed as an insoluble precipitate by addition of 18-crown-6 (0.010 g; 0.038 mmol) to a red solution of $Na(THF)_3^+ 2^-$ (0.033 g; 0.034 mmol) in pentane (3 mL) at room temperature, which dissolved after addition of THF (1 mL). From this solution in 5 d at $-23^\circ C$ dark-blue crystals of the trigallanide $[Na(18-C-6)(THF)_2]^+ [3]^-$ were obtained. – (iii): Obviously, the deep-blue trigallanide **3** formed by reduction of the trigallanyl **3** (see below) in THF with $NaC_{10}H_8$ in THF at room temperature.

Syntheses and Reactions of 3. – (i): A solution of R^*Br (0.672 g; 2.41 mmol) in pentane (10 mL) was added dropwise to a solution

Table 2. Selected parameters of the X-ray structure analyses of the compounds $R^*_4Ga_3^-$ (**3**), $Na(THF)_3^+Ga_2R^*_3^-$ ($M^+ 2^-$) and $[Na(18-C-6)(THF)_2]^+[Ga_3R^*_4]^-$ ($M^+ 3^-$)

	3	$M^+ 2^-$	$M^+ 3^-$
Formula	$C_{48}H_{105}Ga_3Si_4$	$C_{48}H_{105}Ga_2NaO_3Si_3$	$C_{68}H_{148}Ga_3NaO_8Si_4$
M_r	1006.92	977.05	1438.45
System	monoclinic	triclinic	monoclinic
Space group	$C2/c$	$P\bar{1}$	$P2(1)/c$
a [Å]	21.278(2)	12.592(5)	14.9998(2)
b [Å]	12.692(1)	12.6572(5)	20.5701(1)
c [Å]	23.853(2)	19.6557(8)	30.0658(3)
α [°]	90	80.768(1)	90
β [°]	90.212(2)	89.154(1)	92.058(1)
γ [°]	90	68.760(1)	90
V [Å ³]	6442(1)	2879.0(2)	9270.7(2)
Z	4	2	4
D [Mg/m ³]	1.082	1.127	1.108
μ [mm ⁻¹]	1.012	1.039	0.967
$F(000)$	2280	1064	3360
Index range	$-27 \leq h \leq 27$ $-15 \leq k \leq 15$ $-24 \leq l \leq 30$	$-13 \leq h \leq 13$ $-13 \leq k \leq 13$ $-21 \leq l \leq 21$	$-16 \leq h \leq 16$ $-22 \leq k \leq 22$ $-32 \leq l \leq 32$
2θ [°]	3.42–58.42	3.48–46.50	13.62–46.52
Reflections	18377	12733	36480
unique	5554	6645	9921
observed ^[a]	3821	6288	8007
$R(int.)$	0.0540	0.0265	0.0427
x/y ^[b]	1/1	0.1067/ 4.7218	0.1209/ 90.4156
GOOF	1.044	1.076	1.034
$R1$ ^[a]	0.0532	0.0379	0.1016
$wR2$	0.1458	0.1256	0.2476
ρ ^[c]	0.710	0.597	5.696

^[a] $F > 4F(F)$. – ^[b] $w^{-1} = F^2F_o^2 + (xP)^2 + yP$; $P = (F_o^2 + 2F_c^2)/3$. – ^[c] Max. electron density [$e/\text{\AA}^3$].

of $Na(THF)_3^+ 2^0$ (2.353 g; 2.41 mmol) in pentane (15 mL) at -100°C . After 5 h, the mixture was warmed to room temperature. The color of the initially formed deep-blue solution changed finally to deep-green. According to ^1H NMR (exchange of heptane by C_6D_6) and EPR, the solution contained $(R^*)_2$ ^[5] and the radical **3** (the former substance not seen in EPR, the latter not seen in NMR). After removal of the volatile components (ca. 10^{-3} mbar), the residue was placed in pentane (30 mL) and the precipitate (NaBr) removed by filtration. Within 2 months at -23°C , deep-green, air- and moisture-sensitive crystals of **3** (0.412 g; 0.41 mmol; 36%) were formed. – NMR spectra: Not observable. – EPR spectrum: cf. main section. – X-ray structure analysis: cf. Figure 1. – UV/Vis (heptane): $\lambda_{\text{max.}} = 610$ nm. – (ii): The deep-green radical **3** was also formed from $[Na(18-C-6)(THF)_2]^+[3]^-$ (0.086 g; 0.060 mmol) and R^*Br (0.027 g; 0.090 mmol) in C_6D_6 (0.8 mL) within a few days as well as from $[Na(18-C-6)(THF)_2]^+[3]^-$ (0.072 g; 0.050 mmol) and TCNE (0.006 g; 0.05 mmol) in C_6D_6 (0.8 mL) at room temperature immediately. In both cases, the color of the initial dark-blue solutions changed to deep green [cf. (i) for characterization]. – (iii) **Thermolysis of 3**: At 25°C , deep-green **3** in heptane decomposed very slowly into black-blue **2** (observed in EPR) and dark-violet $R^*_4Ga_4$ (observed in NMR).^[6] The mentioned decomposition was complete by heating **3** (0.170 g; 0.169 mmol) for 17 h in heptane (2 mL) at 45°C . After removal of the volatile components (ca. 10^{-3} mbar) and dissolving the residue in pentane (1.5 mL), within 3 d at -23°C dark-blue crystals of the radical **2** were obtained (for another synthesis cf. above, for characterization cf. ref.^[3]). As **2** itself decomposed at higher temperatures under formation of the tetrahedrane **4** besides $(R^*)_2$ (see above), the ther-

molysis of dark-green **3** (0.151 g; 0.150 mmol) in heptane (5 mL) at 100°C led within 3 h exclusively to dark-violet **4**. After removal of the volatile components (ca. 10^{-3} mbar) and dissolving the residue in pentane (3 mL), within 3 d at -23°C dark-violet crystals of **4** (0.075 g; 0.07 mmol; 44%) were obtained (for another synthesis and for characterization see ref.^[4]). Compound **4** is itself very thermostable; the tetrahedrane remains almost undecomposed even after heating a solution in C_6D_{12} for 5 d at 100°C (the NMR spectrum shows only a small amount of R^*D formed). As a solid, **4** does not decompose below 322°C (m.p.).

X-ray Structure Determinations: Siemens SMART Area-detector, Mo- K_α with $\lambda = 0.71073$ Å, $T = 163(2)$ or $193(2)$ K ($R^*_4Ga_2^-$), graphite monochromator, image plate detector, fixed on glass fibre, crystals mounted in perfluoropolyether oil. – Structure determination: The structures were solved by direct methods, SHELX-93. All non-hydrogen atoms were refined anisotropically and H atoms were included in the refinement at calculated positions with a riding model and fixed isotropic U_i values. There is still a large peak in $[Na(18-C-6)(THF)_2]^+[Ga_3R^*_4]^-$ of 5.70 $e/\text{\AA}^3$, 1.02 Å from Ga_3 , that could be due to strong $H\cdots Ga$ and $C\cdots Ga$ contacts between one peripheral methyl group of R^*_2Ga and the anionic Ga atom of the trigallanide $[R^*_2Ga-GaR^*-GaR^*]^-$. The structures of the compounds are shown in Figures 1, 2, and 3, and crystallographic details are summarized in Table 2. Crystallographic data (excluding structure factors) for the structures reported in this paper have been deposited with the Cambridge Crystallographic Data Centre as supplementary publication no. CCDC-152470 (**3**), -152469 $[Na(THF)_3^+ 2^-]$, -152583 $\{[Na(18-C-6)(THF)_2]^+[3]^-]\}$. Copies of

this data can be obtained free of charge on application to CCDC, 12 Union Road, Cambridge CB2 1EZ, UK [Fax: (internat.) + 44-1223/336-033; E-mail: deposit@ccdc.cam.ac.uk].

Acknowledgments

We are grateful to the Deutsche Forschungsgemeinschaft and the Fonds of Chemische Industrie for their generous financial support.

- [1] N. Wiberg, T. Blank, W. Kaim, B. Schwerdeski, G. Linti, *Eur. J. Inorg. Chem.* **2000**, 1475.
- [2] N. Wiberg, K. Amelunxen, T. Blank, H. Nöth, J. Knizek, *Organometallics* **1998**, *17*, 5431.
- [3] N. Wiberg, K. Amelunxen, H. Nöth, H. Schwenk, W. Kaim, A. Klein, T. Scheiring, *Angew. Chem.* **1997**, *109*, 1258; *Angew. Chem. Int. Ed. Engl.* **1997**, *36*, 1213.
- [4] N. Wiberg, K. Amelunxen, H.-W. Lerner, H. Nöth, W. Ponikwar, H. Schwenk, *J. Organomet. Chem.* **1999**, *574*, 246.
- [5] N. Wiberg, K. Amelunxen, H.-W. Lerner, H. Schuster, H. Nöth, I. Krossing, M. Schmidt-Amelunxen, T. Seifert, *J. Organomet. Chem.* **1997**, *542*, 1.
- [6] In addition, $R^*_6Ga_8$ is formed in low yield (*Z. Naturforsch., B*, in preparation). – [6a] W. Uhl, U. Schütz, W. Kaim, E. Waldhör, *J. Organomet. Chem.* **1995**, *501*, 79.
- [7] W. Kaim, *Coord. Chem. Rev.* **1987**, *76*, 187.
- [8] J. A. Weil, J. A. Bolton, J. E. Wertz, *Electron Paramagnetic Resonance*, Wiley, New York, **1994**.
- [9] W. Uhl, K. W. Klinkhammer, M. Layh, W. Massa, *Chem. Ber.* **1991**, *124*, 279.
- [10] W. Uhl, M. Layh, T. Hildenbrand, *J. Organomet. Chem.* **1989**, *364*, 289.
- [11] G. Linti, R. Frey, M. Schmidt, *Z. Naturforsch., Teil B* **1994**, *49*, 958.
- [12] X. He, R. A. Bartlett, M. M. Olmstead, K. Ruhland-Senge, B. E. Sturgeon, P. P. Power, *Angew. Chem.* **1993**, *105*, 761; *Angew. Chem. Int. Ed. Engl.* **1993**, *32*, 717.
- [13] R. D. Schluter, A. H. Cowley, D. A. Atwood, R. A. Jones, M. R. Bernd, C. J. Carrano, *J. Am. Chem. Soc.* **1993**, *115*, 2070.
- [14] A. K. Saxena, H. Zhang, J. A. Maguire, N. S. Hosmane, A. H. Cowley, *Angew. Chem.* **1995**, *107*, 378; *Angew. Chem. Int. Ed. Engl.* **1995**, *34*, 332 and ref. cited herein.
- [15] M. Veith, F. Gotting, S. Becker, V. Huch, *J. Organomet. Chem.* **1991**, *406*, 105.
- [16] A. H. Cowley, A. Decken, C. A. Olazabal, *J. Organomet. Chem.* **1996**, *524*, 271.
- [17] M. Kehwald, W. Köstler, A. Rodig, G. Linti, T. Blank, N. Wiberg, *Organometallics*, **2001**, *20*, 860, and ref. cited herein.
- [18] A. Schnepf, C. Doriat, E. Möllhausen, H. Schnöckel, *Chem. Commun.* **1997**, *21*, 2111.
- [19] J. C. Beamish, R. W. H. Small, I. J. Worrall, *Inorg. Chem.* **1979**, *18*, 220; R. W. H. Small, I. J. Worrall, *Acta Crystallogr. B* **1982**, *38*, 250.
- [20] J. C. Beamish, A. Boardman, R. W. H. Small, I. D. Worrall, *Polyhedron* **1985**, *4*, 983; R. W. H. Small, I. J. Worrall, *Acta Crystallogr. B* **1982**, *38*, 86.
- [21] R. L. Brown, D. Hall, *J. Chem. Soc., Dalton Trans.* **1974**, 988; M. Khan, C. Oldham, M. J. Taylor, D. G. Tuck, *Inorg. Nucl. Chem. Lett.* **1980**, *16*, 469.
- [22] H. J. Cunnning, D. Hall, C. E. Wright, *Cryst. Struct. Commun.* **1974**, *3*, 107; W. Hönl, G. Gerlach, W. Weppner, A. Simon, *J. Solid State Chem.* **1986**, *61*, 171; W. Hönl, A. Simon, *Z. Naturforsch. B* **1986**, *41*, 1391.
- [23] G. Gerlach, W. Hönl, A. Simon, *Z. Anorg. Allg. Chem.* **1982**, *486*, 7.
- [24] J. Su, X.-W. Li, R. C. Crittendon, G. H. Robinson, *Z. Anorg. Allg. Chem.* **1997**, *36*, 5471.
- [25] X.-W. Li, W. T. Pennington, G. H. Robinson, *J. Am. Chem. Soc.* **1995**, *117*, 7578; X.-W. Li, Y. Xie, P. R. Schreiner, K. D. Crippen, R. C. Crittendon, C. F. Campena, H. F. Schaeter, G. H. Robinson, *Organometallics* **1996**, *15*, 3798.
- [26] Holleman-Wiberg, *Lehrbuch der Anorganischen Chemie*, 101st ed., DeGruyter, Berlin, **1995**, p. 1839.
- [27] A. J. Downs (Ed.), *Chemistry of Aluminum, Gallium, Indium and Thallium*, Chapman and Hall, London, **1993**.
- [28] N. Wiberg, T. Blank, H. Schnöckel, F. Möllhausen, unpublished results.
- [29] A. Donchev, A. Schnepf, G. Stöber, E. Baum, H. Schnöckel, T. Blank, N. Wiberg, *Chem. Eur. J.*, in press.
- [30] N. Wiberg, K. Amelunxen, H.-W. Lerner, H. Nöth, J. Knizek, I. Krossing, *Z. Naturforsch., Teil B* **1998**, *53*, 333.
- [31] J. L. Wardell, in: *Comprehensive Organometallic Chemistry* (Eds.: G. Wilkinson, F. G. A. Stone), Pergamon, Oxford **1982**, vol. 1, p. 109.

Received November 21, 2000
[I00445]